

Electromagnetic Launcher Sub-scaling Relationships and Small System Design for Research and Educational Purposes

Heedo Yun

School of Mechanical Engineering, Andong National University, Andong, Kyungbuk 760-749, Korea

(Received 26 April 2000)

Although the electromagnetic launcher technology has been progressed significantly during the past two decades the number of firing test facilities are not many. This is probably due to the large budget and man power required to build and maintain full scale electromagnetic launcher facilities. As the EM launcher technology's potential capabilities have been somewhat demonstrated with the full scale large systems the research is now headed more toward overcoming specific difficulties and answering questions experimentally with smaller, cost effective systems. The first half of this paper presents EM launcher's improved sub-scaling relationships based upon magnetic, thermal and momentum differential equations and EM launcher's basic equations. With the proposed scaling method the field variables can be matched or scaled linearly between the two geometrically scaled systems. The second half of the paper presents pulsed power system's circuit analysis and design technique, which is applied to the capacitor-powered small pulsed power system with crow-barring circuitry. The effect of the so-called speed volt is included. A sub-scaled small system's design is provided as an example.

1. Introduction

Since the pioneering work of Rashleigh and Marshall who accelerated a 3 gram lexan projectile to a muzzle velocity of 5.9 km/s in a 4 meter long electromagnetic launcher (EML) in 1978 [1], the EM launcher technology has received significant attention from the U.S. and a few other countries. With the main focus on improving the tank gun's firing power with the EML technology, large experimental firing facilities were quickly funded, designed and fabricated in the late 1970s in Texas (Univ. Texas, Austin, 90 mm bore EM launcher, powered by homopolar generator and large inductors [2]) and in California (Maxwell, Green Farm, 90 mm bore EM launcher powered by a bank of capacitors [3]). Test firings in these facilities have somewhat demonstrated the potential capability of the electromagnetic launcher technology and also helped researchers learn of several difficulties which had to be overcome before applying the technology to a practical use. These difficulties include the understanding and improving the solid armature-rail sliding interface physics [4], plasma armature's behavior at the projectile velocity over 3-5 km/s range [5], characterizing the material's behavior under the electromagnetic, thermal and mechanical extreme conditions [6], the velocity skin effect, the rail wear and gouging, the armature transitionings, and the demand for more compact pulsed power technology. The electromagnetic launcher research is now headed more toward overcoming specific difficulties and answering questions with small,

cost-effective systems. When properly sub-scaled, the small system can reproduce identical muzzle velocity, magnetic, thermal and mechanical stress fields as the full scale system's, therefore enabling direct correlation to the large system. These systems can be built in a small laboratory or even on a table top.

The first half of this paper describes an improved scaling method for the sub-scale system design which accurately correlates the two geometrically scaled systems. The second half of the paper presents the pulsed power circuit analyses for the sub-scale system. Closed form approximate solutions for the current profile including the so-called speed volt effect and crow barring circuitry was obtained using perturbation technique. Overall system's efficiency was addressed. A small system design is presented as an example case.

2. EM Launcher Scaling Relationships

In order to match the magnetic, thermal and stress fields between the two different systems the time scale factor (K_t) must be equal to the square of the geometric scale factor (K_x), and the gun current scale factor (K_I) must be equal to K_x [8]. With this scaling the launch package's mass is scaled by a scale factor of K_x^3 , the acceleration by $1/K_x$, the muzzle velocity by K_x , the gun effective length by K_x^3 , and the muzzle kinetic energy by K_x^5 . This method is useful in the sense that the magnetic, thermal and stress fields are duplicated in the sub-scale model. However, this method can not be uti-

lized for the cases where the muzzle velocity on the order of the full scale system's is required in the scaled model (such as the cases for testing the rail wear/gouging phenomena). In this publication the matching scaling method reported in [8] is extended to a more general one. The electrical, thermal and mechanical properties of the gun component materials are not changed in the scaling.

2.1. Derivations

Scaling relationships are derived based upon the magnetic, thermal and momentum partial differential equations and a few basic EM launcher equations [7]. The magnetic diffusion equations for the full scale system are

$$\nabla \times \frac{B}{\mu} = J, \quad (1)$$

$$\nabla \times \frac{J}{\sigma} = -\frac{\partial B}{\partial t}, \quad (2)$$

$$\nabla \cdot B = 0, \quad (3)$$

where B is the magnetic flux density, J the electrical current density, t time, σ the electrical conductivity and μ the permeability. The thermal diffusion equation which describes the temperature field and the ohmic heat generation is

$$\nabla \cdot k \nabla T + \frac{J \cdot J}{\sigma} = C_p \frac{\partial T}{\partial t}, \quad (4)$$

where T is the temperature, k the thermal conductivity and C_p the volumetric specific heat. The momentum equation which describes the stress field and the Lorentz body force generation is

$$\nabla \cdot S + J \times B = \rho a, \quad (5)$$

where S is the stress tensor, ρ the material density and a the acceleration. The basic EM launcher equations used are

$$F = m a = p A \equiv \frac{1}{2} L' I^2, \quad (6)$$

$$v \equiv \frac{1}{m} \int \frac{1}{2} L' I^2 dt, \quad (7)$$

$$l \equiv \frac{1}{m} \iint \frac{1}{2} L' I^2 dt dt, \quad (8)$$

$$E = \frac{1}{2} m v^2, \quad (9)$$

$$q = \frac{1}{2 \mu_0} B^2, \quad (10)$$

where F is the driving force acting on the armature, m the launch package total mass, p the average bore pressure, A the gun bore area, L' the gun's inductance gradient value, I the gun current, v the launch package's muzzle exit velocity, l the gun effective length, E the launch package's kinetic energy at the time of muzzle exit, and q is the average magnetic repulsive pressure on the rail face.

Equations for the scaled system are derived by change of variables. Unprimed letters, (), denote the full scale system's variables, while primed letters, ('), denote the sub-scale system's variables (except for the gun inductance gradient value, L' , which is unchanged by the geometric scaling). The constant scale factor, K , describes the scaling and is defined as (') = K (), i.e. $B' = K_B B$, and etc.. With this notation the equations for the sub-scale system can be written as

$$\nabla' \times \frac{B'}{\mu} = \frac{K_B}{K_x K_J} J', \quad (1')$$

$$\nabla' \times \frac{J'}{\sigma} = -\frac{K_J K_t}{K_x K_B} \frac{\partial B'}{\partial t'}, \quad (2')$$

$$\nabla' \cdot B' = 0, \quad (3')$$

$$\frac{K_J K_x^2}{K_T} \nabla' \cdot k \nabla' T' + \frac{J' \cdot J'}{\sigma} = \frac{K_J K_t}{K_T} C_p \frac{\partial T'}{\partial t'}, \quad (4')$$

$$\frac{K_J K_B K_x}{K_S} \nabla' \cdot S' + J' \times B' = \frac{K_J K_b K_x^3}{K_a K_m} \rho' a', \quad (5')$$

$$\frac{K_l^2}{K_F} F' = \frac{K_l^2}{K_m K_a} m' a' = \frac{K_l^2}{K_p K_x^2} p' A' \equiv \frac{1}{2} L' I'^2, \quad (6')$$

$$v' \equiv \frac{K_v K_m}{K_l^2 K_t} \frac{1}{m'} \int \frac{1}{2} L' I'^2 dt', \quad (7')$$

$$l' \equiv \frac{K_l K_m}{K_l^2 K_t^2} \frac{1}{m'} \iint \frac{1}{2} L' I'^2 dt' dt', \quad (8')$$

$$E' = \frac{K_E}{K_m K_v} \frac{1}{2} m' v'^2, \quad (9')$$

$$q' = \frac{K_q}{K_B^2 2 \mu_0} B'^2. \quad (10')$$

The Eqs. (1)~(10) should satisfy the same laws of physics which are described for the full scale system in (1)~(10) in order for the scaled system to be a real physical system. This requires that each coefficient of the above equations (consisting of the K 's only) must be equal to a unity. These requirements can be summarized as

$$K_t = K_x^2, \quad (11)$$

$$K_B = \frac{K_l}{K_x}, \quad (12)$$

$$K_J = \frac{K_l}{K_x^2}, \quad (13)$$

$$K_a = \frac{K_l^2}{K_m}, \quad (14)$$

$$K_s = \frac{K_I^2}{K_x^2}, \quad (15)$$

$$K_F = K_I^2, \quad (16)$$

$$K_p = \frac{K_I^2}{K_x^2}, \quad (17)$$

$$K_q = \frac{K_I^2}{K_x^2}, \quad (18)$$

$$K_I = \frac{K_I^2 K_I}{K_x^4} = \frac{K_I^2}{K_x^2}, \quad (19)$$

$$K_v = \frac{K_I^2 K_I}{K_m} = \frac{K_I^2 K_x^2}{K_m}, \quad (20)$$

$$K_l = \frac{K_I^2 K_I^2}{K_m} = \frac{K_I^2 K_x^4}{K_m}, \quad (21)$$

$$K_E = \frac{K_I^4 K_I^2}{K_m} = \frac{K_I^4 K_x^4}{K_m}. \quad (22)$$

The geometric scale factor K_x , the launch package mass scale factor K_m , and the gun current scale factor K_I are the input scale factors, whereas the 12 scale factors which appear on the left hand side of (11)–(22) are the outputs. As shown by (11) the time scale factor K_t is required to be the square of the K_x in order for the scaling relationships to be a linear one (i.e., constant scale factors). This is rather a strong design restriction. Note that in (5)' the launch package mass is scaled by scaling the package density. The last term of (4)' was used to obtain the left part of (19), so that the conduction term (the first term of (4)') can be neglected in the approximate solution in the non-linear scaling cases.

If the prescribed input scale factors do not satisfy (11), then either one of the differential Eqs. (1)' or (2)' violates the laws of physics. This means that the initial assumption of linear scaling is no longer valid and some of the scale factors are, in general, functions of x and t (instead of being constants). Eqs. (1)'–(5)' must be re-written accordingly. Solving the non-linear scaling equations seems to be not a good idea as it is practically impossible. Instead, the non-linear cases are solved approximately, in the average sense, using (12)–(18) and the left part of (19)–(22), where K_I is treated as the fourth independent input scale factor.

The above derivation assumes that the material properties are temperature independent. Average material property values for the temperature range of interest may be used in cases of non-matching temperature field. One may attempt to further improve the scaling relationships by expressing the electrical conductivity as $\sigma = \sigma_0(1 + c T) = \sigma_0(1 + c T'/K_T)$ in (2)' and (4)', and etc.. This modification can improve

the accuracy of the scaling, but is not recommended because of its mathematical complexity. Using the average material property values is more practical, although the results may not be very accurate.

If all the launch package dimensions are scaled by the geometric scale factor, K_x , then the launch package mass is scaled by K_x^3 ($K_m = K_x^3$). In this publication, however, K_m is treated as an independent scale factor by assuming that the armature dimensions are scaled by K_x , while the dimensions of the rest of the package are scaled independently. Therefore, the package mass can be chosen arbitrarily (this was roughly reflected in the last term of (5)'). This assumption can violate the momentum Eq. (5)', and the resulting stress field of the launch package may not scale linearly.

2.2. Applications

Once the input scale factors K_x , K_m and K_I are prescribed, the twelve output scale factors can be derived by (11)–(22). All variables scale linearly, i.e., constant scale factors. Designers have the freedom of arbitrarily prescribing the three independent input scale factors, whichever set serves their scaling goals best.

Identical B , T , and S field results are possible in the scaled system if we choose that $K_I = K_x$. Only two scale factors K_x and K_m are the arbitrary inputs. In this case, J is scaled by $1/K_x$, a by K_x^2/K_m , F by K_x^2 , p and q are matched, v is scaled by K_x^4/K_m , l by K_x^6/K_m and E by K_x^8/K_m . The matching case of [8] is a special case of this with an additional requirement that $K_m = K_x^3$.

Identical muzzle velocity, in addition to the identical B , T , and S field results can be achieved if we further choose that $K_m = K_x^4$, in addition to that $K_I = K_x$. Only one scale factor K_x remains as the arbitrary input. In this case, J is scaled by $1/K_x$, a by $1/K_x^2$, F by K_x^2 , p and q are matched, l is scaled by K_x^2 and E by K_x^4 . This method is probably the most beneficial choice as most of the important gun parameters are matched between the full and the sub-scale systems.

Identical acceleration, in addition to the identical B , T , and S field results can be achieved if we choose that $K_m = K_x^2$, in addition to that $K_I = K_x$. Only one scale factor K_x remains as the arbitrary input. In this case, J is scaled by $1/K_x$, F by K_x^2 , p and q are matched, v is scaled by K_x^2 , l by K_x^4 and E by K_x^6 .

The following example demonstrates how the differences in the material properties between the two systems can affect the scaled equations. When the electrical conductivity values differ between the two systems, for example, (2)' and (11) can be rewritten as

$$\nabla' \times \frac{J'}{\sigma} = -\frac{K_I}{K_\sigma K_x^2} \frac{\partial B'}{\partial t'}, \quad (23)$$

$$K_I = K_\sigma K_x^2. \quad (24)$$

Intentionally scaling the material properties can be a very difficult task, as finding the conductor materials of the right

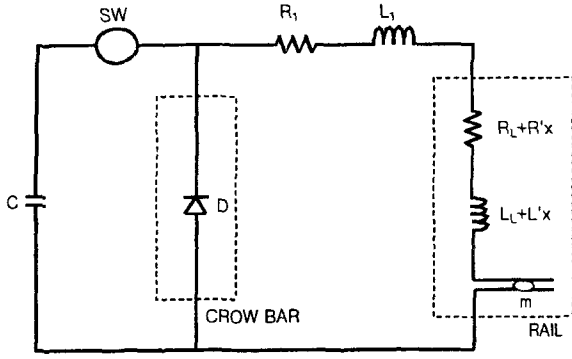


Fig. 1. Equivalent circuit diagram.

electrical conductivity is difficult, or practically impossible.

3. Pulsed Power Circuit Analysis

We consider a capacitor powered pulsed power supply system which powers a sub-scaled electromagnetic launcher. The equivalent circuit consists of a capacitor, electromagnetic launcher, switch, crow bar diode, resistors and inductors, as shown in the Fig. 1.

For the outer loop in the diagram the Kirchhoff's voltage law is:

$$L \frac{d^2 Q}{dt^2} + (R + L'v) \frac{dQ}{dt} + \frac{1}{C} Q = 0, \quad (25)$$

where Q is the capacitor charge; L' is the rail inductance gradient, $(dL/dt) = (dL/dx) (dx/dt) = L'v$, and $L = L_1 + L_L + L'x$, etc.. The energy conservation is:

$$\frac{1}{2C} Q^2 + \int R I^2 dt + \frac{1}{2} L I^2 + \frac{1}{2} m v^2 = \frac{1}{2C} Q_0^2, \quad (26)$$

where Q_0 is the capacitor charge at $t=0$. Differentiating (26) and using (25), we get the formula of the electromagnetic launcher driving force:

$$f = ma = \frac{1}{2} L' I^2, \quad (27)$$

which states that the driving force is proportional to the rail inductance gradient L' and the square of the gun current I . L' is essentially constant along the gun length. Projectile's velocity and position data may be obtained by integrating the acceleration data.

$$v = \frac{1}{2m} \int I^2 dt \quad (28)$$

Solution of the nonlinear Eq. (25) (with v expressed in (28)) can be obtained numerically. In the following the perturbation technique is used to obtain an approximate solution of (25) in a closed form. The solution is used for the circuit analysis later in the paper.

At the beginning of the launch the projectile velocity is

relatively low and the so-called speed resistance term $L'v$ may be neglected in (25). Solutions of the resulting differential equation of constant coefficients are:

$$I = Q_0 \omega \frac{1}{\sqrt{1 - \zeta^2}} e^{-\zeta \omega t} \sin \omega_d t, \quad (29)$$

$$v = \frac{L' Q_0^2 \omega}{8m} \left[\frac{(1 - e^{-2\zeta \omega t})}{\zeta} - \frac{2e^{-2\zeta \omega t} \sin(\omega_d t) \cos(\omega_d t - \phi)}{1 - \zeta^2} \right] \quad (30)$$

where

$$\omega = 1/\sqrt{LC}, \quad \omega_d = \omega \sqrt{1 - \zeta^2}, \quad (31a-b)$$

$$\zeta = 0.5R\sqrt{C/L}, \quad \phi = \tan^{-1} \frac{\zeta}{\sqrt{1 - \zeta^2}}. \quad (31c-d)$$

The first peak current occurs at the time $\omega_d t = (\pi/2) - \phi$. The first zero-voltage crossing occurs at the time $\omega_d t = (\pi/2) + \phi$. Because the ζ values are small in the typical electromagnetic launcher applications we may employ approximate solutions t_0 , I_0 , and v_0 at the first zero-volt crossing as follows:

$$\omega t_0 = \frac{\pi}{2}, \quad (32a)$$

$$I_0 = Q_0 \omega e^{-\frac{\pi}{2}\zeta}, \quad (32b)$$

$$v_0 = \frac{L' Q_0^2 \omega}{8m\zeta} [1 - e^{-\pi\zeta}]. \quad (32c)$$

The switch opens at the first zero-volt crossing and the current is directed to the crow bar diode circuit. For $t > t_0$, the Kirchhoff's voltage law states:

$$L \frac{dI}{dt} + (R + L'v) I = 0. \quad (33)$$

Perturbation technique is used to obtain an approximate solution. We start with the solution of the linearized equation of (33), i.e., the term $L'v$ is removed:

$$I_1 = I_0 e^{-\frac{R}{L}(t-t_0)}, \quad (34a)$$

$$v_1 = v_0 + \frac{L' I_0^2 L}{4mR} \left[1 - e^{-\frac{2R}{L}(t-t_0)} \right] \\ = \frac{L' Q_0^2 \omega}{8m\zeta} [1 - e^{-\zeta \{ \pi + 4\omega(t-t_0) \}}] \quad (34b)$$

We define a correction ε to the current such that $I = I_1 + \varepsilon$ and rewrite (33) with approximation that $v = v_1$.

$$L \frac{d\varepsilon}{dt} + (R + L'v_1) \varepsilon = -L'v_1 I_1, \quad (35)$$

where ε is the amount of current reduced due to the presence of the speed resistance term $L'v$. Solution of (35) yields the approximate solution for $t > t_0$:

$$I = \left[Q_0 \omega e^{-\frac{\pi}{2}\zeta} \right] \left[e^{-\frac{R}{L}(t-t_0)} \right] \left[e^{-s \left(n + \frac{1}{2} e^{-2n} - \frac{1}{2} \right)} \right] \quad (36)$$

$$n = \frac{R}{L}(t - t_0) = 2\zeta\omega(t - t_0), \quad (37a)$$

$$s = \frac{L'v_*}{R}, \quad v_* = \frac{L'Q_0^2\omega}{8m\zeta} = \frac{L'E_s}{2mR}, \quad (37b-c)$$

where v_* is a reference velocity parameter which is obtained by letting $t \rightarrow \infty$ in (30) or in (34b). Actual projectile velocity is always lower than this, thus v_* is an upper bound. The projectile velocity is calculated by numerical integration in (28) with the current given in (36). The calculated gun current and the projectile velocity data are summarized in Fig. 2 and Fig. 3. s is the normalized speed resistance parameter.

The pulsed power system's efficiency is defined as the ratio of the muzzle kinetic energy to the initial capacitor stored energy.

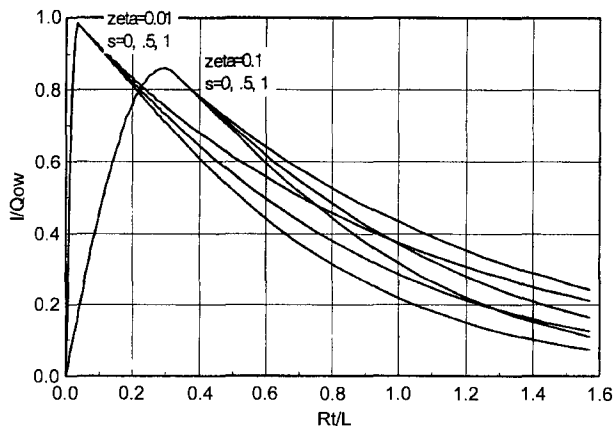


Fig. 2. Current profile for different values of damping ratio ζ and speed resistance parameter s .

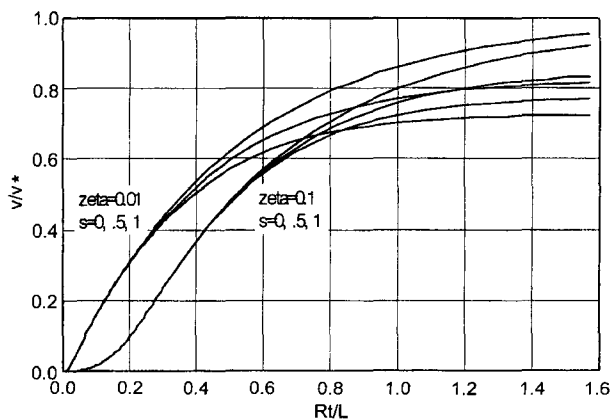


Fig. 3. Velocity profile for different values of damping ratio ζ and speed resistance parameter s .

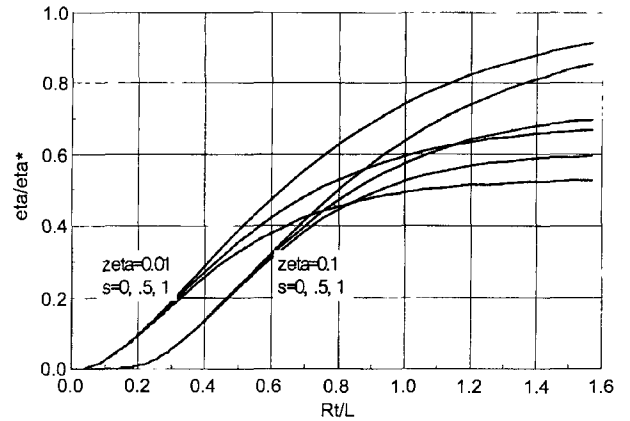


Fig. 4. Pulsed power system's energy efficiency for different values of damping ratio ζ and speed resistance parameter s .

$$\eta = \frac{mv_*^2/2}{Q_0^2/2C} \quad (38)$$

The corresponding reference efficiency for the velocity upper limit v_* is defined.

$$\eta_* = \frac{mv_*^2/2}{Q_0^2/2C} = \frac{L'^2 E_s}{8mR^2} = \frac{1}{4}s. \quad (39)$$

Actual system efficiency is always lower than this, thus η_* is an upper bound. The calculated efficiency data is summarized in Fig. 4 for different values of damping ratio ζ and the speed resistance parameter s . It is shown that the speed resistance can greatly hinder the system's performance.

4. Small System Design

A 90 mm round bore, high L' , composite laminated electromagnetic launcher was successfully constructed for the 9 MJ range gun system at the CEM-UT in 1993 [9]. The goal of the program was to demonstrate the repetitive firings of 9 MJ kinetic energy shots out of the electromagnetic launcher at the rate of 3 rpm for 3 minutes. Prior to the completion of the launcher, a 30 mm bore sub-scale version was built and tested at the CEM-UT to verify the system's

Table 1. 90 mm/30 mm bore CEM-UT launchers

bore dia	90	30	mm
peak current	2,600	717	kA
exit time	8.	2.	ms
launch package mass	4,150	77	g
muzzle velocity	2,083	2,080	m/s
effective launcher length	7.0	1.89	m
muzzle kinetic energy	9,000	167	kJ
launcher L'	0.49	0.49	μ H/m
reference	[12]	[11, 13]	

Table 2. Linear 1/3 scaling of 90 mm bore launcher

bore dia	90	30	mm
peak current	2,600	867	kA
exit time	8.	0.89	ms
launch package mass	4,150	51.2	g
muzzle velocity	2,083	2,083	m/s
effective launcher length	7.0	0.78	m
muzzle kinetic energy	9,000	110	kJ
peak acceleration	40	360	kgee
launcher L'	0.49	0.49	H/m
bore pressure	260	260	MPa

performance and to develop construction techniques [10, 11]. The scaling parameters used are listed in Table 1 [11, 12, 13].

In the CEM-UT's design the time scale factor (0.250) was not the square of the geometric scale factor (0.333), thus the scaling was not linear and the correlations of the sub-scale test results were valid in the average sense only. Scale factors of output data obtained experimentally from both guns in the average sense matched well with the calculations done with the left hand equations of (11)~(22) as predicted.

Table 2 lists the linear 1/3 scale model parameters of the same launcher. Eqn. (11)~(22) were used. The 1/3 scale model provides identical magnetic, temperature and stress distributions as well as identical muzzle velocities as for the full scale system.

Design parameters of the pulsed power system for the sub-scale model can be selected using the results obtained in the section III. For the purpose of demonstrating how the algorithm works we choose that the capacitance $C = 0.017$ F and the damping ratio $\zeta = 0.1$. We calculate that $Q_0\omega = 1.014$ MA from (32.b) and the peak current requirement in Table 2, $v_* = 12.13 Q_0$ from (37.c), and $Rt/L = 180.3/Q_0$. Now iteration is required to determine the values of Q_0 and ω . We start with an initial guess of $v/v_* = 0.6$. Then, we calculate that $v_* = 3,477$ m/s, $Q_0 = 286.6$ C, $Rt/L = 0.629$, and $Q_0 = 286.6$, $Rt/L = 0.629$, $\omega = 3,538$ 1/s, $L = 4.7$ μ H and $R = 3.33$ m Ω . We calculate $s = 0.512$ from (37b) and we find the new value $v/v_* = 0.58$ from the data in Fig. 3. The new velocity is $v = 0.58$, $v_* = 2,017$ m/s. This velocity is approx. 3% lower than the desired value of 2,083 m/s. To improve the solution we repeat the above calculation with a new guess $v/v_* = 0.58$. We calculate that $v_* = 3,591$ m/s, $Q_0 = 296$ C, $Rt/L = 0.61$, $\omega = 3,426$ 1/s, $L = 5.01$ μ H, $R = 3.43$ m Ω , $s = 0.513$ and $v/v_* = 0.579$ and $v = 2,080$ m/s. The calculated parameters satisfy all the requirements listed in Table 2, thus the calculation is completed. The system's efficiency can be calculated from (38). $\eta = 111$ kJ/2,577 kJ = 4.3%. The low efficiency number is due to the high damping ratio we selected at the beginning of the design process. Most of the capacitor energy is wasted in the Ohmic heating. The numerical data chosen for the above example case were for the demonstration purpose only. One may want to reduce

the circuit resistance in order to improve the system efficiency.

5. Conclusions

The linear scaling relationships of electromagnetic launchers were derived based upon the magnetic, thermal and momentum equations and a few EML equations. The developed scaling system can provide matching magnetic, thermal and mechanical stress field as well as a matching muzzle velocity between the two geometrically scaled systems.

The governing differential equation of the EML pulsed power circuit is nonlinear due to the presence of the speed resistance term. Using the perturbation technique, a closed form approximate solution was obtained for the current profile while including the speed resistance effect. It was shown analytically that the speed resistance hinders the system's performance significantly.

Linear 1/3 scaling results of the CEM-UT's 90 mm EML system was provided as an example. Pulsed power system design for the resulting 30 mm bore system was provided for demonstration.

Acknowledgments

Research funding for this work was provided by the Andong National University under the 1998 contract "High efficiency small electromagnetic launcher system development for the research and educational purposes."

References

- [1] S. C. Rashleigh and R. A. Marshall, Electromagnetic Acceleration of Macroparticles to High Velocity, *J. Appl. Phys.*, **49**, 2540-2542 (1978).
- [2] D. R. Peterson, et al., Design and Operation of a High-Energy Railgun Facility, *IEEE Trans. Magnetics*, **25**(1), Jan., 438-442 (1989).
- [3] D. Haugh, et al., Large Caliber Armature Firings at Green Farm Electric Gun Test Facility, *IEEE Trans. Magnetics*, **33**(1), Jan., 68-73 (1997).
- [4] C. Persad, Solid Armature Performance: A Progress Review 1980-1990, *IEEE Trans. Magnetics*, **33**(1), Jan., 134-139 (1997).
- [5] E. M. Drobyshevski, et al., Experiments on Simple Railgun with the Copacted Plasma Armature, *IEEE Trans. Magnetics*, **31**(1), Jan., 295-298 (1995).
- [6] R. C. Zowarka, H. D. Yun, and A. Alexander, Railgun solid armature scaling model, *IEEE Trans. Magnetics*, **33**(1), January, 169-174 (1997).
- [7] H. D. Yun, EM Gun Scaling Relationships, *IEEE Trans. Magnetics*, **35**(1), Jan., 484-488 (1999).
- [8] K. T. Hsieh and B. K. Kim, One kind of scaling relations on electromechanical systems, *IEEE Trans. Magnetics*, **33**(1), January, 240-244 (1997).
- [9] J. D. Herbst, Installation and Commissioning of the 9 MJ

- Range Gun System 90 mm High L' Laminated Railgun, *IEEE Trans. Magnetism*, **33**(1), January, 554-559 (1997).
- [10] R. L. Laughlin, J. L. Bacon, R. C. Zowarka, and J. H. Price, Design, Analysis, and Fabrication of Two Lightweight, High L' Railguns, *IEEE Trans. Magnetism*, **29**(1), January, 451-456 (1993).
- [11] J. J. Hahne, J. H. Herbst, and J. L. Upshaw, Fabrication and testing of a 30 mm and 90 mm laminated, high L' railgun design and built at CEM-UT, *IEEE Trans. Magnetism*, **31**(1), January, 303-308 (1995).
- [12] J. D. Herbst, B. Rech, R. F. Thelen, and R. C. Thompson Status of the 9 MJ range gun system, *IEEE Trans. Magn.* **31**(1), January, 540-545 (1995).
- [13] J. H. Price and H. D. Yun, Design and testing of integrated metal armature sabots for launch of armor penetrating projectiles from electric guns, *IEEE Trans. Magn.* **31**(1), January, 219-224 (1995).